ISBN: 978-3-95450-132-8 doi:10.18429/JACoW-IPAC2014-WEPME026

LAYOUT OF THE VACUUM SYSTEM FOR A NEW ESRF STORAGE RING

M. Hahn, J.C. Biasci, H.P. Marques, ESRF, Grenoble, France

Abstract

The proposed 7-bend achromat lattice for the new 6 GeV electron storage ring of the European Synchrotron Radiation Facility imposes a change of the entire vacuum system. Small bore magnets will require low conductance vacuum chambers. Conventional vacuum pumps will have to be assisted by distributed pumping provided by Non-Evaporable Getter (NEG) coating. The time constraints for design, prototyping, pre-assembly, installation and commissioning of the new systems require simple solutions and the use of existing expertise where possible. In this paper the draft layout of the vacuum system will be explained, information about the expected dynamic pressure distribution and conditioning will be given. Some technical solutions to resolve specific issues arising from the small vacuum chamber dimensions and the dense arrangement of components are described.

INTRODUCTION

The lattice of the new machine has been designed following the multiple bend achromat (MBA) concepts as described by Einfeld et al. [1] while taking into account the physical limitation of an existing storage ring tunnel and the need to preserve the 32-fold symmetry and useable length of the insertion device sector of five meters [2]. This results in a hybrid multi-bend achromat (HMBA) lattice, the main parameters relevant for the vacuum system are given in Table 1:

Table 1: HMBA Lattice Storage Ring Main Parameters

Parameter	Unit	Value
Beam Energy, E	GeV	6
Design current, I	mA	200
Total photon flux from bending magnets at design current Φ_p	Ph/s	$9.7 \cdot 10^{20}$
Total power from bending magnets at design current P_T	kW	534

THE STORAGE RING VACUUM SYSTEM

Following the symmetry of the lattice, the vacuum system of the storage ring is divided into 32 cells, out of which 2 are defined as injection cells and therefore slightly different in terms of geometry and location of the absorbers and power generation (+4%). Each of the vacuum cells is isolated from the next by a pneumatic full metal gate valve, a 2nd pneumatic valve divides each cell into two independent vacuum sectors by isolating the insertion device straight section. Seven bending magnets per cell generate synchrotron radiation, there are three central magnets (combined dipole/ quadrupole) of 0.538 T and 0.427 T respectively and four outer magnets with a magnetic field varying from 0.17 T to 0.64 T (decrease or increase) in five segments. The succession of these magnets of a standard cell is shown in Fig. 1.

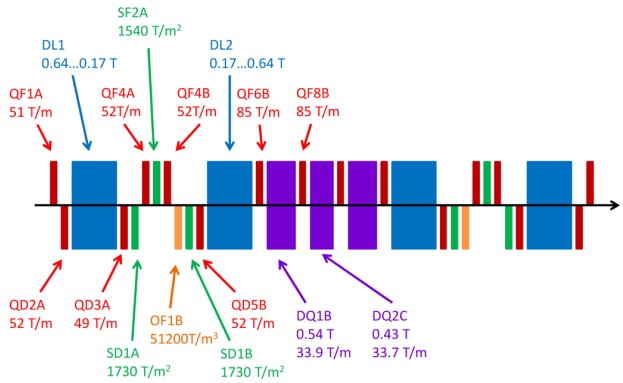

Figure 1: Magnet position and strength of HBMA lattice.

Vacuum Chambers

The required field strength especially of the central multi-pole magnets requires a small bore size of the magnet leading to a small cross section of the vacuum chamber. Most of the chambers will be composed of an electron beam transport chamber and antechamber on which lumped photon absorbers, ultra high vacuum (UHV) pumps and vacuum gauges will be installed. Advantages of the concept are described in [3]. The small gap in most of the magnets in the horizontal plan requires a limited vertical height of the part of the chamber connecting the antechamber to the beam-chamber therefore the resistance of the profile against collapsing is an issue. Among copper, aluminium extrusion and stainless steel only the latter can provide the required stiffness with sheet thickness as low as 2mm, stainless steel 316LN has therefore been proposed as principal construction material for the vacuum chamber.

The standard lattice cell has been logically divided into a central and an upstream/downstream part (Fig. 2); different beam stay clear requirements and bore size of the multipole magnets define two different areas in terms of principal geometry of the e-beam vacuum chamber: The proposed beam stay clear is ±8.3 mm / ±5.5 mm (hor. /vert.) for the central and ±15.0 mm / ±10.0 mm (hor. /vert.) for the cell upstream and downstream part. Figure 3 shows a typical upstream part vacuum chamber with the electron beam chamber on the right and the antechamber on the left.

ISBN: 978-3-95450-132-8 doi:10.18429/JACoW-IPAC2014-WEPME026

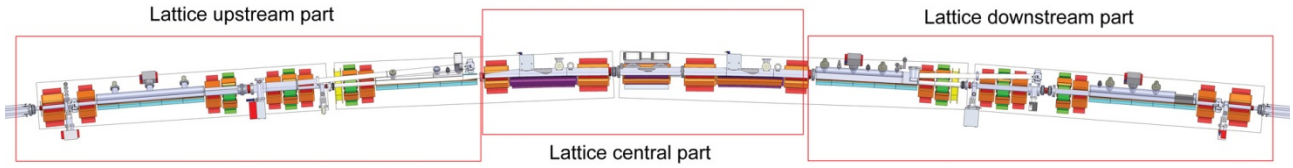

Figure 2: Engineering layout of the HMBA lattice cell with central and upstream/downstream part.

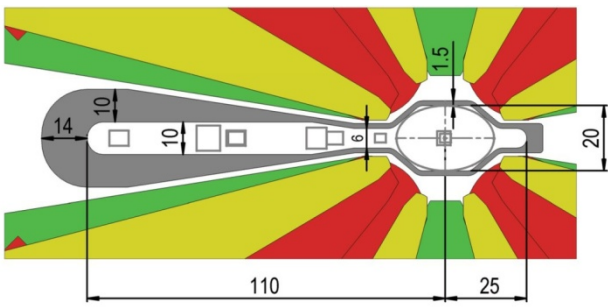

Figure3: Upstream vacuum chamber with antechamber.

The lumped absorbers are distributed all around the circumference of the storage ring. They will receive the entire bending magnet radiation as the former ESRF bending magnet beamlines are going to receive photons from a dedicated short insertion device in the central part of the lattice. The construction material for the absorbers is going to be mainly oxygen-free copper. The potential option to operate the machine with higher current will require the use of alumina-reinforced alloys like Glidcop® for some of these absorbers to cope with the higher power density. Figure 4 shows the vacuum chamber profile designed for the central part of the cell.

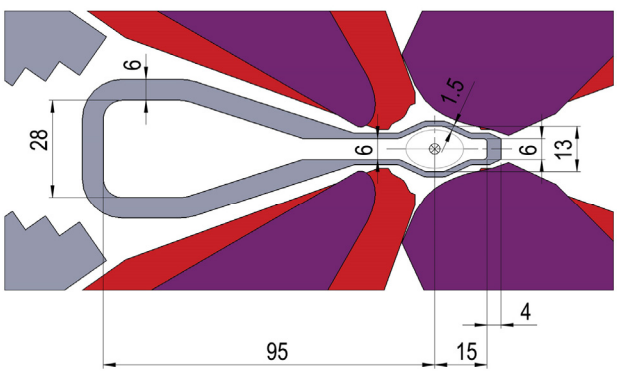

Figure 4: Central vacuum chamber profile.

Stainless steel Flanges according to the Conflat® standard will connect the vacuum chambers, the existing NEG-coated aluminium ID vacuum chambers [4] are equipped with explosion bonded aluminium to stainless steel flanges.

Vacuum Pumps

It is planned to re-use a large fraction of the UHV pumps of the existing storage ring. Accordingly the pumping concept of the new machine will be based on sputtering ion pumps and cartridge based NEG pumps. NEG-coatings will be used on the insertion device (ID) sector for the ID chamber itself and the previous and following vacuum chamber.

Vacuum Bake-out

The installation procedure which foresees to connect the chambers segment by segment in the tunnel is not compatible with bringing and keeping the chambers under vacuum during the assembly. The operation of an in-situ baking system will allow for a good base pressure. Due to the different cross sections of the vacuum chambers the choice and application method for the baking pads and ribbons needs to be optimised for each case. The radiation level inside the tunnel will be significantly higher than today due to inter-bunch scattering (Touschek effect) so the baking materials which stay permanently on the chambers will be have to be qualified in terms of radiation resistance. The fixed wiring of the connection of the electrical heaters to the control electronics will allow to start the bake quickly by remote and avoid also breakage of connectors which may occur with repetitive connection and disconnection of mobile bake control carts.

Vacuum Instrumentation

The layout of UHV pumps, total pressure gauges and residual gas analysers (RGA) is shown on Fig. 5. It is planned to continue the use of thermal conductivity gauges of the Pirani type for the low vacuum and Penning inverted magnetron gauges for the High vacuum and UHV. Due to the low vacuum conductance of most of the chambers the pressure will vary significantly along the beam path, the pressure readout of the ion pump controllers will be used as additional pressure gauges.

Residual gas analysers will be installed in each of the 64 vacuum sectors.

ISBN: 978-3-95450-132-8 doi:10.18429/JACoW-IPAC2014-WEPME026

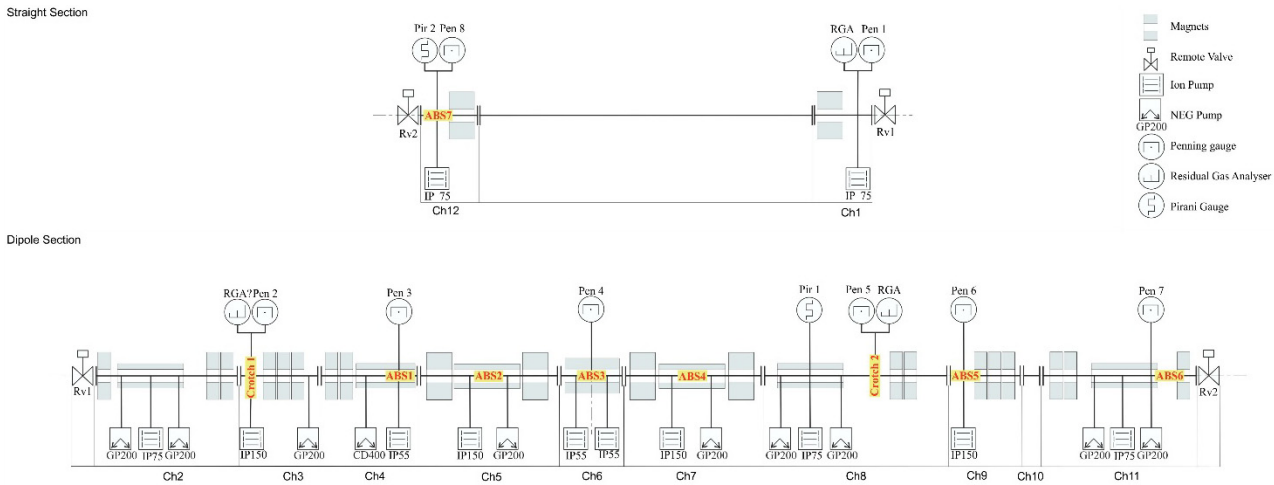

Figure 5: Vacuum instrumentation layout.

VACUUM SIMULATION

Vacuum simulations have been carried out with a conductance-based approach, the main gas source being the photon stimulated desorption (PSD) from the lumped absorbers. The expected pressure distribution of a new standard cell after 3000Ah of beam conditioning is shown in Fig. 6. Vacuum Conditioning data from the photodesorption measurement beamline D31 at ESRF [5] has been used to simulate the evolution of the peak pressure and the average pressure.

The pressure bump which can be seen on the right of the plot is developing over the flat ID vessel due to the 1.3 kW of synchrotron radiation which will be absorbed there.

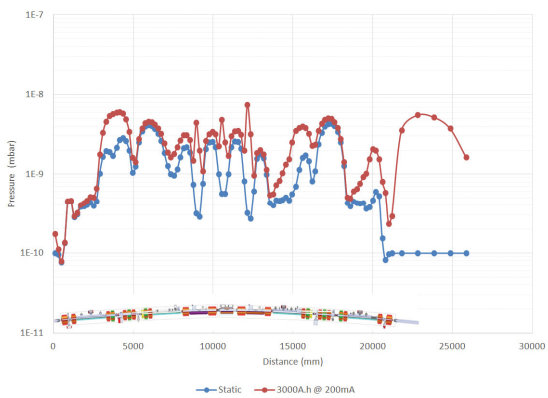

Figure 6: Pressure distribution of a new standard cell.

In order to reduce the integral pressure along the insertion device straight section the vacuum chambers connected to the extremity of the ID chamber will be NEG coated.

Under the assumption to keep the dynamic pressure in the 10^{-7} mbar range which preserves the UHV pumps the electron beam current has been gradually increased up to the design current of 200 mA in the simulation shown in Fig. 7.

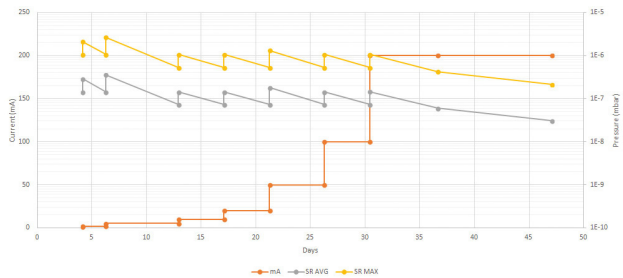

Figure 7: Ramping of the electron beam current in function of maximum (yellow) and average(grey) vacuum pressure.

NEXT STEPS

The feasibility of the vacuum chamber construction is going to be verified by ordering of prototypes. Tests of the bake-out equipment will be carried out, the homogeneity of the temperature distribution on the chamber profile will be measured. The chamber profile of the upstream and downstream ID vacuum chambers will be frozen to design the NEG coating setup for deposition and to start discussions with valve suppliers for the design of the RF contact of the sector valves.

REFERENCES

[1] D. Einfeld, et al., “Design of a Diffraction Limited Light Source (DIFL)” PAC’95, Dallas, p. 177; http://www.JACoW.org

[2] J.L. Revol, et al., “ESRF Upgrade Phase II”, IPAC’13, Shanghai, p. 1140.

[3] E. Al-Dmour, et al., “The Vacuum System for the Spanish Synchrotron Light Source (ALBA)”, EPAC’06 ,Edingburgh, p. 3398.

[4] M. Hahn et al., “Status of NEG coating at ESRF”, PAC’05, Knoxville, p. 422.

[5] H.P. Marques, et al., “Photodesorption Measurements at ESRF D31” IPAC’11, San Sebastian, p. 1518.